Conflict of Interest

European Journal of Radiology – Research Article

Clinical impact of low tube voltage computed tomography during hepatic arteriography with low iodine to detect hepatocellular carcinoma before transarterial chemoembolization

Akitoshi Inoue—Nothing to declare

Ryo Uemura—Nothing to declare

Kai Takaki—Nothing to declare

Akinaga Sonoda—Nothing to declare

Shinichi Ota—Nothing to declare

Norihisa Nitta—Nothing to declare

Bolorkhand Batsaikhan—Nothing to declare

Hiroaki Takahashi—Nothing to declare

Yoshiyuki Watanabe—Nothing to declare

European Journal of Radiology – Research Article

Clinical impact of low tube voltage computed tomography during hepatic arteriography with low iodine to detect hepatocellular carcinoma before transarterial chemoembolization

Akitoshi Inoue[1] (ORCID: 0000-0002-8610-2571), Ryo Uemura[1], Kai Takaki[1], Akinaga Sonoda[1], Shinichi Ota[1], Norihisa Nitta[1], Bolorkhand Batsaikhan[2], Hiroaki Takahashi[3] (ORCID: 0000-0002-8731-0081), Yoshiyuki Watanabe[1] (ORCID: 0000-0003-3906-3730)

1) Department of Radiology, Shiga University of Medical Science, Shiga, Japan

2) Department of Radiology, Breast Care Center, Ulaanbaatar, Mongolia

3) Department of Radiology, Mayo Clinic, Rochester, U.S.A.

Corresponding author: Akitoshi Inoue (ORCID: 0000-0002-8610-2571)

Department of Radiology, Shiga University of Medical Science

Seta, Tsukinowa-cho, Otsu, Shiga, 520-2192, Japan

Phone No: +81-77-548-2288

Fax No: +81-77-548-2536

Email Address: akino@belle.shiga-med.ac.jp

Author Contributions

Conceptualization—Akitoshi Inoue, Norihisa Nitta

Methodology—Akitoshi Inoue, Hiroaki Takahashi

Image interpretation—Ryo Uemura, Kai Takaki, Akinaga Sonoda

Image review for reference standard—Shinichi Ota

Image analysis (CT number measurement)—Bolorkhand Batsaikhan

Statistical analysis—Akitoshi Inoue, Hiroaki Takahashi

Writing original draft preparation—Akitoshi Inoue

Surpervision—Yoshiyuki Watanabe

Conflict of Interest

No potential conflict of interest was reported by the authors.

This study is not funded by any organization.

European Journal of Radiology–Research article

Clinical impact of low tube voltage computed tomography during hepatic arteriography with low iodine to detect hepatocellular carcinoma before transarterial chemoembolization

Abstract

Purpose: This study aimed to evaluate the clinical impact of low tube voltage computed tomography (CT) during hepatic arteriography (CTHA) using low iodine contrast to detect hepatocellular carcinoma (HCC).

Materials and methods: CTHA images were obtained using a dual-spin technique (80 kVp and 135 kVp) with 30 ml of low-dose iodine contrast (75 mgI/ml). Three radiologists reviewed 135 kVp and 80 kVp CTHA images to diagnose HCC, recording their confidence scores and evaluations of sharpness, noise, artifact, and overall image quality. Lesion-to-liver contrast ratios and objective noise were measured by a non-reader radiologist.

Results: We included 23 patients (body mass index, 23.6 ± 2.6 kg/m^2) with 89 HCCs. The mean radiation dose index volume was 21.3 mGy at 135 kVp and 9.4 mGy at 80 kVp ($P < 0.001$). The overall sensitivity and positive predictive value for diagnosing HCCs at 80 kVp vs. 135 kVp were 0.787 vs. 0.730 and 0.712 vs. 0.756, respectively. The lesion-to-liver contrast ratio at 80 kVp was significantly higher than at 135 kVp in the first (3.1 vs. 2.0; $P = 0.008$) and second phase (3.1 vs. 2.3; $P = 0.016$). Objective noise was significantly higher at 80 kVp than at 135 kVp in the first (15. 6 ± 4.9 vs. 11.0 ± 3.1; $P < 0.001$) and second (16.9 ± 5.2 vs. 15.0 ± 7.3; $P = 0.046$) phases.

Conclusion: An 80 kVp CTHA, with lower-dose iodine, improved the sensitivity and reduced the radiation dose, despite a decreased positive predictive value in comparison with a 135-kVp CTHA with the same iodine dose.

Key words

Computed tomography; Hepatocellular carcinoma; Chemoembolization; Contrast media; Radiation Dosage

List of abbreviations

BMI: body mass index

CT: computed tomography

$CTDI_{vol}$: CT dose index volume

CTHA: computed tomography during arteriography

DLP: dose-length product

FROC: free-response receiver operating characteristic curves

HCC; hepatocellular carcinoma

LI-RADS: liver imaging reporting and data system

LLF: lesion localization fraction

NLF: non-lesion localization fraction

PC-AKI: post-contrast acute kidney injury

PPV: positive predictive value

TACE: transarterial chemoembolization

Introduction

Hepatocellular carcinoma (HCC) has been identified as the most common type of primary neoplasm in the liver and the fourth most common cause of cancer-related death worldwide [1]. Antiviral therapy to eliminate the hepatitis virus, which is the most common etiology of chronic liver disease causing HCC, has a high success rate. However, in the United States, liver cancer is increasing rapidly because most infected people remain undiagnosed; moreover, it can also be due to other preventable risk factors, such as obesity, alcohol, and smoking [2]. The therapeutic strategy for HCCs depends on liver function and disease staging. Transarterial chemoembolization (TACE), combined with various anticancer agents and additional procedures, is an established therapeutic procedure for unresectable HCCs [3-8].

To achieve tumor control and a preferable patient outcome with TACE, it is essential to identify HCCs. Digital subtraction angiography, involving tumor staining, is widely used to detect HCCs. Despite its higher radiation dose and amount of iodine contrast media, CT during hepatic arteriography (CTHA) has high detectability for HCC [9-11].

However, CTHA has been associated with two potential problems. First, post-contrast acute kidney injury (PC-AKI) may arise due to an overload of the iodine contrast media administrated in TACE procedures [12]. An increased creatinine level (by ≥ 0.5 mg/dl or $\geq 25\%$ from baseline within 72 hours after TACE) was observed in 2.6%–9% of patients; a few required transient hemodialysis [13-15]. Second, CTHA delivers additional radiation over that of the TACE procedure and routine follow-up CT exams. Most patients with HCCs are associated with chronic liver disease; they are recommended to undergo imaging surveillance to detect HCCs in the early stage [16] and are

treated with multiple TACE sessions [17], resulting in the accumulation of their lifetime radiation exposure.

In low tube voltages, the photoelectric effect in X-ray attenuation is increased, especially for a relatively high effective atomic number, including iodine. As a result, the attenuation of iodine is increased in low tube voltage scan [18]. According to this physics background, the low tube voltage scan is a known technique that provides higher contrast enhancement of the scan [19]. Several clinical studies have demonstrated the benefit of low tube voltage scans in abdominal solid-organ evaluation [20], CT venography for the detection of deep vein thrombosis (with higher contrast enhancement) [21], CT urography [22], CT enterography [23], CT colonography [24], and vascular imaging (with reduced radiation dose) [25]. Because HCC is a hyper-enhancing liver tumor, low tube voltage (80–100 kVp) scans in intravenous contrast-enhanced CT allow a reduction in the iodine load without reducing image quality and diagnostic accuracy compared with a standard tube voltage contrast-enhanced CT scan with intravenous iodine [26-31]. However, no researchers to date have investigated how a low tube voltage scan affects CTHA in detecting HCC. Thus, in this study, we aimed to evaluate the diagnostic accuracy and reader confidence, as well as image quality, using low tube voltage CTHA, with low levels of iodine contrast, for the detection of HCCs before TACE, compared with standard tube voltage CTHA.

Methods

Patients

This retrospective study was approved by our institutional review board. Written informed consent was waived. A non-reader radiologist (A.I.) screened and retrospectively enrolled patients with HCC who underwent TACE from January

2018 to March 2019. Medical chart review extracted patient demographics, including age, sex, body weight, height, and body mass index (BMI). The exclusion criteria were as follows: patients with >10 suspicious lesions, incomplete CTHA examination, no low tube voltage (80 kVp) scan, CTHA obtained in multiple TACE sessions during the enrollment period, no CTHA performed with injection via the common hepatic artery, presence of lipiodol accumulation, no pre-contrast scan, and lack of a reference standard.

CT acquisition

All procedures and scans were conducted using a hybrid CT/angiography system (Aquilion ONE, Canon Medical Systems, Tochigi, Japan). A 5-Fr sheath (25 cm; Supersheath; Medikit, Tokyo, Japan) was introduced into the right femoral artery; then, a 5-Fr catheter (70 cm; J-shaped; Terumo Clinical Supply, Tokyo, Japan) was carried to the superior mesenteric artery for CT scan during portography.

A catheter was placed in the common hepatic artery, and then CTHA was scanned at 5 and 15 seconds after intra-arterial administration of 30 ml of fourfold diluted iopamidol (75 mgI/ml) (iopamiron 300 mgI/ml, Bayer Yakuhin, Osaka, Japan) at the rate of 2 ml/sec through the catheter. The reduced iodine dose was determined as half of the clinical routine dose (30 ml of iodine contrast media [150 mgI/ml]), which is lower than those used in previous CTHA studies [10-11]. The CT acquisition parameters were as follows: tube current, automatic exposure control (SD14), maximum 550 mA at 80 kVp; tube potential, 135 kVp and 80 kVp; and rotation time, 0.5 seconds. The reconstruction parameters were as follows: slice thickness/increment, 3/3 mm; reconstruction field of view, 320 mm; reconstruction technique, AIDR 3D (mild strength); and matrix size, 512 × 512. Each slice was scanned alternately at 135 kVp and 80 kVp, in that order,

and the interval of two scans in each slice was approximately 1 s. In other words, the X-ray tube and detector rotated twice at the same location to obtain two different tube voltages. We decided to scan using a combination of tube voltage with larger difference (135/80 kVp) because the CT scanner allowed the selection of 135/100 or 135/80 kVp.

CT interpretation

Three abdominal radiologists (R.U., T.K., and A.S., with 5, 11, and 22 years of experience of abdominal imaging, respectively), blinded to CT acquisition and reconstruction parameters, reviewed the 80 kVp or 135 kVp CT images in two reading sessions on diagnostic quality monitors. They were allowed to adjust the window setting. They were asked to detect enhanced lesions suspected as HCC, record the location (liver segment, series number, and slice number), and capture an image in JPEG format to match the reference standard. They rated the possibility of HCC on a confidence scale from 0 to 100 (0–24, probable non-HCC; 25–50, could not rule out HCC; 51–75, probable HCC; 76–100, definite HCC). They were informed that a cutoff of 25 would be used for diagnostic performance analysis. Subsequently, they subjectively recorded overall image quality (a 5-point Likert score), artifact (a 4-point Likert score), sharpness (a 3-point Likert score), and noise (a 3-point Likert score) (**Table 1**). Either 80 kVp or 135 kVp CT images were shown once in the same session (the same case was never shown). In the third session, 80 kVp and 135 kVp images were randomly displayed, and the reader radiologists blinded to the image tube voltage compared both the images in a side-by-side fashion and recorded a 5-point comparison rating for the evaluation of the liver parenchyma (subjective impression combining of texture, attenuation, and noise) and detection of the HCCs (−2, right image was obviously worse; −1, right image was slightly

worse; 0, both images were comparable; +1, right image was slightly better; +2, right image was obviously better). All examinations were anonymized and randomized; each reading session was made 3 weeks apart to wash out recall bias.

Objective measurements

A non-reader radiologist (BB, with 3 years of experience in abdominal imaging) measured the maximum diameter of HCC, as defined by the reference standard. The radiologist measured the CT number of HCCs using a circular region of interest (ROI) that was set as large as possible (100 mm^2) to cover the whole tumor at the slice, with maximum tumor diameter and CT numbers of the liver parenchyma, while avoiding vessels and the bile duct. The standard deviation of the CT number in the subcutaneous fat was taken as a measurement of noise, using a circular ROI as large as possible, depending on the patient's body size. The lesion-to-liver contrast ratio was calculated using the following formula.

$$Lesion\ to\ liver\ contrast\ ratio = \frac{HU_{HCC} - HU_{liver}}{HU_{liver}}$$

Reference standard

Another non-reader radiologist (S.O.), with 27 years of experience in abdominal imaging, reviewed the preoperative or follow-up CT/MR images within 2 months of the CTHA procedure to rate the category as defined by the Liver Imaging Reporting and Data System (LI-LADS) [32] and to interpret CTAP/CTHA and non-contrast CT after TACE. LI-RADS 4/5 lesions on preoperative or follow-up CT/MRI and LI-RADS 3 lesions with a defect on CTAP or lipiodol accumulation after TACE were defined as HCCs. The

reference reader recorded the HCC location (segment, numbers of series, and slice of HCC) and captured the images in JPEG format. Another non-reader radiologist (AI), with 12 years of experience in abdominal imaging, matched the reading session results with the reference standards by viewing the scans, as well as the captured JPEG images. HCC diagnosis was judged "true positive" if lesions that were recorded with a confidence score ≥25 matched the reference standard. HCC diagnosis was judged "false positive" if lesions that were recorded with a confidence score ≥25 did not match any reference standard. HCC diagnosis was judged "false negative" if the readers did not identify lesions or rated them with a confidence score <25.

Statistical analysis

Lesion sensitivity and positive predictive value (PPV) with 95% confidence intervals (CIs) were calculated based on the reader's binary results, defined by a confidence score cutoff of 25. If the CIs did not overlap the 95% CI between the 135 kVp and 80 kVp scans, a significant difference was then considered. Specificity and negative predictive value could not be calculated because there were no control cases.

Free-response receiver operating characteristic curves (FROC) were employed to assess reader performance in respect to the confidence score. FROC is a subtype of the receiver operating characteristic curve (ROC), with the false positive rate plotted on the x-axis and sensitivity on the y-axis. The FROC curve was plotted with non-lesion localization fraction (NLF) on the x-axis and lesion localization fraction (LLF) on the y-axis. NLF is defined as the cumulative number of non-lesion localizations divided by the total number of cases. LLF is defined as the cumulative number of lesion localizations divided by the total number of lesions. The value of LLF at a confidence score of 25 was

equal to the abovementioned sensitivity. A maximal LLF value of 0 indicates lesion detectability. The range of LLF is 0–1; however, NLF may exceed 1.0. Therefore, the FROC analysis was only used to visualize the diagnostic performance and confidence scores and not to derive a figure of merit.

The Likert scale scores and comparison scores of subjective image quality in 135 kVp and 80 kVp scans were compared using the Wilcoxon signed-rank test. In the analysis, post-hoc correction was performed for the comparison of the scores. Noise and tumor-to-liver contrast rates were compared using paired t-tests. In these metrics, a p-value of <0.05 was considered to be a significant difference. The statistical analysis was performed using RStudio software (version 4.0.3; R Project for Statistical Computing, Vienna, Austria).

Results

In total, 53 patients with HCCs underwent TACE; however, 32 patients were excluded because they had >10 HCCs, (n = 6), incomplete scan range in at least one series (n = 5), no 80 kVp scan (n = 5), multiple TACE sessions in the enrollment period (n = 4), contrast media injected via the segmental or subsegmental artery (not the common hepatic artery) for CTHA (n = 4), the existence of lipiodol accumulation (n = 2), no pre-contrast scan (n = 2), and lack of standard reference (n = 2). Finally, 23 patients (mean age, 74.4 ± 8.0 years; male/female, 17/6; BMI, 23.6 ± 2.6 kg/m^2) with 89 HCCs (mean diameter, 13.1 ± 2.6 mm) were enrolled in this study (**Fig. 1**). The patients demonstrated one (n = 3), two (n = 5), three (n = 7), four (n = 1), five (n = 1), six (n = 2), seven (n = 1), eight (n = 1), nine (n = 1), or ten (n = 1) reference standard HCC lesions (**Table 2**). The iodine amount per body weight was 38.7 ± 6.49 mgI/kg. The mean CT dose index volume ($CTDI_{vol}$) and dose-length product (DLP) at 135 kVp were 21.3 mGy and 341.1 mGy cm, respectively. In 80 kVp scans, they

were found to be significantly lower: $CTDI_{vol}$, 9.4 mGy ($P < 0.01$); DLP, 149.7 mGy cm ($P < 0.001$). The values in all 80 kVp scans were the same (in all cases) because the tube current reached the manufacturer's limitation of 550 mA.

Overall sensitivity was higher in the 80 kVp images than in the 135 kVp images (0.787 vs. 0.730); the overall PPV was lower in the 80 kVp images than in the 135 kVp images (0.712 vs. 0.756). Regarding the readers, sensitivity was improved in two of the three readers (R1, 0.831 vs. 0.730; R3, 0.764 vs. 0.674), whereas PPV was degraded (R1, 0.712 vs. 0,783; R3, 0.756 vs. 0.759). In one of the three readers, both sensitivity and PPV decreased (R2, sensitivity: 0.764 vs. 0.787, PPV: 0.673 vs. 0.729) (**Table 3**; **Figs. 2–3**). In the FROC analysis, maximum LLFs were higher in 80 kVp images than in 135 kVp images for two of the three readers, which suggested that 80 kVp images offer higher detectability for HCCs. LLF was similar in both images for one of the three readers. The curves of the 80 kVp images for all readers tended more to the right side (greater NLF), which implies that the 80 kVp scan gives more frequent false positives, taking into account the reader's confidence (**Fig. 4**).

In independent subjective image quality analysis, no significant difference was noted in the artifact and overall image quality. However, the same reader rated a higher score of sharpness in 80 kVp images than in 135 kVp images (2.3 ± 0.5 vs. 2.1 ± 0.3; $P = 0.008$) and a lower noise score in 80 kVp images than in 135 kVp images (2.1 ± 0.3 vs. 2.7 ± 0.5; $P = 0.002$) (**Table 4**). In one of three readers, a positive score was rated for detecting HCCs ($P = 0.018$), whereas a negative score was rated for evaluating liver parenchyma ($P = 0.035$) (**Fig. 5**). The relationship between the scores for detecting HCC and for evaluating liver parenchyma demonstrated a tendency toward trade-off in two of the three readers (R1, 12 cases with positive score in detecting HCC vs. 12 cases with negative score in evaluating liver parenchyma; R2, 10 cases with positive

score in detecting HCC vs. 14 cases with negative score in evaluating liver parenchyma) (Fig. 6a and b).

The lesion-to-liver contrast ratio was significantly greater in the 80 kVp images than in the 135 kV images, both in the first (3.1 vs. 2.0; P = 0.007) and second phase (3.1 vs. 2.3; P = 0.016). The objective noise was significantly higher at 80 kVp images than at 135 kVp images in the first (15. 6 ± 4.9 vs. 11.0 ± 3.1; P < 0.001) and second (16.9 ± 5.2 vs. 15.0 ± 7.3; P=0.046) phases (**Table 5**).

Discussion

This multi-reader study has compared the diagnostic accuracy and subjective and objective image quality between 135 kVp and 80 kVp images, seeking verification of low tube voltage CTHA scans with lower-dose iodine (75 mgI/ml) compared with routine clinical protocol (150 mgI/ml) in non-obese patients (BMI: 23.6 ± 2.6 kg/m^2). CTHA implemented with a tube voltage of 80 kVp and half-dose iodine improved the sensitivity for detecting HCCs (0.787 vs. 0.730) with significantly higher lesion-to-liver contrast despite higher image noise. When the reader's confidence for HCCs was considered (using FROC curves), two of the three readers found higher sensitivity.

In 80 kVp images, sensitivity was increased, whereas PPV was decreased. In other words, additional true lesions were revealed, but false positives increased at the same time. Intrahepatic shunts and wedge- or triangular-shaped lesions, as well as HCCs, are frequently seen in CTHA for chronic liver disease. Consequently, contrast effects for both pathologies are boosted in 80 kVp images. In the low tube voltage scan, the average photon energy decreases and approaches the k-edge of iodine, resulting in a larger proportion of photon interactions with iodine via the photoelectric effect,

causing a higher attenuation of the X-ray beam and higher contrast enhancement [19]. Thus, the results of this study are compatible with the principle of a low tube voltage scan.

In subjective image quality, no significant difference was seen in the overall image quality and artifact. However, one reader recorded a greater degree of noise in 80 kVp images. Similarly, objective noise was significantly greater in 80 kVp images. Iterative reconstruction is helpful to de-noise in low tube voltage scans [27, 30]; our study implemented AIDR 3D. However, excessive low tube voltage, relative to body size, can deteriorate the diagnostic utility of the image due to severe noise [19]. Our study enrolled non-obese patients (mean BMI, 23.6 kg/m^2), similar to previous studies (mean BMI, 22.2–24 kg/m^2) [27, 28, 30, 31]. It is essential to realize that notable noise in low tube voltage scans may deteriorate the diagnostic performance for large-sized patients.

We employed an iodine dose (30 ml, 75 mgI/ml) half that of the routine clinical protocol (30 ml, 150 mgI/ml) and lower than those in previous studies [9, 10] but did not compare different doses to explore the optimal dose for 135 kVp and 80 kVp scans. Previous studies have demonstrated that a low tube voltage scan facilitates the reduction of iodine in contrast-enhanced CT for diagnosing HCCs. A tube voltage of 100 kVp enabled a 20% reduction of iodine dose, with higher tumor-to-liver contrast, in patients with estimated glomerular filtration rate <60 $ml/min/m^2$ [26]. An 80 kVp scan enabled a 33% reduction of the iodine dose without compromising diagnostic performance [27]. Given that the diagnostic performances at 135 kVp and 80 kVp are comparable, further iodine dose reduction is potentially possible for 80 kVp scans. Although the risk of PC-AKI in intra-arterial administration without first-pass renal exposure is the same as with intravenous administration, a higher risk of PC-AKI during first-pass renal exposure involves backflow from the celiac artery and its branch

during TACE procedure [12]. In summary, reducing the iodine dose is potentially more important in CTHA; thus, a low tube voltage scan is helpful for CTHA.

Another benefit of a low tube voltage scan is lower radiation dose. Our study showed significantly lower radiation dose parameters in the 80 kVp scan in the non-obese patients; however, it is unknown for obese patients. Despite increased noise, diagnostic performance was not significantly different from the standard tube voltage scan. Most patients with HCCs have chronic liver disease and are recommended to undergo imaging surveillance to detect HCCs in the early stage [16]. They are treated with multiple TACE sessions [17], resulting in accumulated radiation exposure. Radiation dose reduction is therefore essential in patients undergoing TACE. A low tube voltage (80 kVp) scan can facilitate reduction of the iodine load and, thus, the radiation dose in CTHA; however, a further study is warranted for patients who are obese.

This study has some limitations. First, this study included patients with small to medium build (BMI, 23.6 ± 2.6 kg/m^2) but not patients with obesity. Generally, a higher radiation dose is required to obtain optimal image quality in large-sized patients, but the maximum tube current is 550 mA in the 80 kVp scan used in this study. An 80 kVp image obtained from the same scanner as used in this study would not be useful for large-sized patients due to degraded image quality. Second, scan timings at 80 kVp and 135 kVp were not identical, as both image sets were acquired by sequential scan. However, the difference in scan timing in each set was considered too little (approximately 1 s) to affect contrast enhancement. Third, the number of patients was relatively small, but a considerable number of HCCs were evaluated, since some patients had several HCCs. Fourth, we did not enroll control patients without HCCs because all patients who underwent CTHA were planned to be treated with TACE for HCCs. Patient-level analysis was not available; therefore, specificity, negative

predictive value, and accuracy could not be calculated at a per-lesion level. ROC analysis was not recommended for the same reason. Instead, we utilized FROC analysis, but features such as the area under the curve and figure of merit were not recommended [33]. Fifth, a substantial number of patients were excluded because of strict inclusion and exclusion criteria designed to eliminate complicated cases (e.g., numerous HCCs in a single patient, viable lesion masked by lipiodol accumulation). Sixth, only one iodine concentration (75 mgI/ml) was evaluated, as multiple iodine concentrations would not be acceptable from an ethical perspective. Finally, morphologic characteristics have been determined to be important for differentiating HCC from intrahepatic shunts. To diagnose HCC in clinical practice, it is essential to compare CTHA findings with the findings of available cross-sectional imaging examinations before TACE; however, the readers were asked to interpret only CTHA. As a result, the diagnostic performance might be lower than real-world values.

In conclusion, low tube voltage CTHA, using a reduced amount of iodine contrast media, improved the detectability of HCCs and demonstrated a significantly higher lesion-to-liver contrast ratio without compromising subjective image quality, although the number of false positives increased in comparison with a 135-kVp CTHA with the same iodine dose. A low tube voltage scan is beneficial in CTHA for revealing mildly enhanced HCCs and reducing the risk of PC-AKI.

Declarations

Ethics approval and consent to participate

This retrospective study was approved by our institutional review board. The need for a written informed consent was waived.

Funding

This study was not funded.

References

[1] A. Villanueva, Hepatocellular Carcinoma, N Engl J Med 380(15) (2019) 1450-1462.

[2] R.L. Siegel, K.D. Miller, A. Jemal, Cancer statistics, 2020, CA Cancer J Clin 70(1) (2020) 7-30.

[3] R. Yamada, M. Sato, M. Kawabata, H. Nakatsuka, K. Nakamura, S. Takashima, Hepatic artery embolization in 120 patients with unresectable hepatoma, Radiology 148 (1982) 397-401.

[4] S. Miyayama, O. Matsui, M. Yamashiro, Y. Ryu, K. Kaito, K. Ozaki, T. Takeda, N. Yoneda, K. Notsumata, D. Toya, N. Tanaka, T. Mitsui, Ultraselective transcatheter arterial chemoembolization with a 2-f tip microcatheter for small hepatocellular carcinomas: relationship between local tumor recurrence and visualization of the portal vein with iodized oil, J Vasc Interv Radiol 18(3) (2007) 365-76.

[5] T. Irie, N. Takahashi, T. Kamoshida, Balloon-Occluded Trans-Arterial Chemoembolization Technique with Alternate Infusion of Cisplatin and Gelatin Slurry for Small Hepatocellular Carcinoma Nodules Adjacent to the Glisson Sheath, Biomed Res Int 2019 (2019) 8350926.

[6] A. Inoue, S. Ota, K. Takaki, Y. Imai, S. Sato, S. Watanabe, Y. Tomozawa, T. Iwai, Y. Murakami, A. Sonoda, N. Nitta, K. Murata, Change in hepatic hemodynamics assessed by hepatic arterial blood pressure and computed tomography during hepatic angiography with the double balloon technique, Jpn J Radiol 37(6) (2019) 487-493.

[7] R. Loffroy, M. Ronot, M. Greget, A. Bouvier, C. Mastier, C. Sengel, L. Tselikas, D. Arnold, G. Maleux, J.P. Pelage, O. Pellerin, B. Peynircioglu, B. Sangro, N. Schaefer, M. Urdaniz, N. Kaufmann, J.I. Bilbao, T. Helmberger, V. Vilgrain, C.-F.P. Investigators, Short-term Safety and Quality of Life Outcomes Following Radioembolization in Primary and Secondary Liver Tumours: a Multi-centre Analysis of 200 Patients in France, Cardiovasc Intervent Radiol 44(1) (2021) 36-49.

[8] A. Imamura, H. Taguchi, H. Takano, H. Funatsu, K. Nakamura, H. Arimitsu, S. Chiba, Whole-liver transcatheter arterial chemoinfusion and bland embolization with fine-powder cisplatin and trisacryl gelatin microspheres for treating unresectable multiple hepatocellular carcinoma, Jpn J Radiol 39(5) (2021) 494-502.

[9] O. Makita, Y. Yamashita, A. Arakawa, Y. Nakayama, K. Mitsuzaki, M. Ando, T. Namimoto, M. Takahashi, Diagnostic accuracy of helical CT arterial portography and CT hepatic arteriography for hypervascular

hepatocellular carcinoma in chronic liver damage. An ROC analysis, Acta Radiol 5(41) (2000) 464-469.

[10] M. Tsurusaki, K. Sugimoto, M. Fujii, T. Fukuda, S. Matsumoto, K. Sugimura, Combination of CT during arterial portography and double-phase CT hepatic arteriography with multi-detector row helical CT for evaluation of hypervascular hepatocellular carcinoma, Clin Radiol 62(12) (2007) 1189-97.

[11] T. Murakami, H. Oi, M. Hori, T. Kim, S. Takahashi, K. Tomoda, Y. Narumi, H. Nakamura, Helical CT during arterial portography and hepatic arteriography for detecting hypervascular hepatocellular carcinoma, AJR Am J Roentgenol 169(1) (1997) 131-135.

[12] A.J. van der Molen, P. Reimer, I.A. Dekkers, G. Bongartz, M.F. Bellin, M. Bertolotto, O. Clement, G. Heinz-Peer, F. Stacul, J.A.W. Webb, H.S. Thomsen, Post-contrast acute kidney injury - Part 1: Definition, clinical features, incidence, role of contrast medium and risk factors: Recommendations for updated ESUR Contrast Medium Safety Committee guidelines, Eur Radiol 28(7) (2018) 2845-2855.

[13] K. Hayakawa, M. Tanikake, T. Kirishima, N. Yoshinami, H. Shintani, E. Yamamoto, T. Morimoto, The incidence of contrast-induced nephropathy (CIN) following transarterial chemoembolisation (TACE) in patients with hepatocellular carcinoma (HCC), Eur Radiol 24(5) (2014) 1105-11.

[14] H.S. Cho, J.W. Seo, Y. Kang, E.J. Bae, H.J. Kim, S.H. Chang, D.J. Park, Incidence and risk factors for radiocontrast-induced nephropathy in patients with hepatocellular carcinoma undergoing transcatheter arterial chemoembolization, Clin Exp Nephrol 15(5) (2011) 714-719.

[15] M. Aoe, T. Kanemitsu, T. Ohki, S. Kishi, Y. Ogura, Y. Takenaka, T. Hashiba, H. Ambe, E. Furukawa, Y. Kurata, M. Ichikawa, K. Ohara, T. Honda, S. Furuse, K. Saito, N. Toda, N. Mise, Incidence and risk factors of contrast-induced nephropathy after transcatheter arterial chemoembolization in hepatocellular carcinoma, Clin Exp Nephrol 23(9) (2019) 1141-1146.

[16] Y.E. Chung, M.J. Kim, M.S. Park, J.Y. Choi, J.S. Lim, K.A. Kim, K.W. Kim, The impact of CT follow-up interval on stages of hepatocellular carcinomas detected during the surveillance of patients with liver cirrhosis, AJR Am J Roentgenol 199(4) (2012) 816-21.

[17] J.A. White, D.T. Redden, M.K. Bryant, D. Dorn, S. Saddekni, A.K. Abdel Aal, J. Zarzour, D. Bolus, J.K. Smith, S. Gray, D.E. Eckhoff, D.A. DuBay, Predictors of repeat transarterial chemoembolization in the treatment of hepatocellular carcinoma, HPB (Oxford) 16(12) (2014) 1095-101.

[18] Y. Nakayama, K Awai, Funama Y, et al. Abdominal CT with low tube voltage: preliminary observations about radiation dose, contrast enhancement, image quality, and noise. Radiology. 237: 945-951. 2005.

[19] A.R. Seyal, A. Arslanoglu, S.F. Abboud, A. Sahin, J.M. Horowitz, V. Yaghmai, CT of the Abdomen with Reduced Tube Voltage in Adults: A Practical Approach, Radiographics 35(7) (2015) 1922-1939.

[20] G.A. Zamboni, M.C. Ambrosetti, S. Guariglia, C. Cavedon, R. Pozzi Mucelli, Single-energy low-voltage arterial phase MDCT scanning increases conspicuity of adenocarcinoma of the pancreas, Eur J Radiol 83(3) (2014) e113-7.

[21] S. Ichikawa, T. Ichikawa, U. Motosugi, A. Imaizumi, K. Sano, H. Morisaka, Computed tomography (CT) venography with dual-energy CT: low tube voltage and dose reduction of contrast medium for detection of deep vein thrombosis, 38(5) (2014) 797-801.

[22] A.B. Shinagare, V.A. Sahni, C.A. Sadow, S.M. Erturk, S.G. Silverman, Feasibility of low-tube-voltage excretory phase images during CT urography: assessment using a dual-energy CT scanner, AJR Am J Roentgenol 197(5) (2011) 1146-51.

[23] L.S. Guimaraes, J.G. Fletcher, L. Yu, J.E. Huprich, J.L. Fidler, A. Manduca, J.C. Ramirez-Giraldo, D.R. Holmes, Jr., C.H. McCollough, Feasibility of dose reduction using novel denoising techniques for low kV (80 kV) CT enterography: optimization and validation, Acad Radiol 17(10) (2010) 1203-10.

[24] K.J. Chang, D.B. Caovan, D.J. Grand, W. Huda, W.W. Mayo-Smith, Reducing radiation dose at CT colonography: decreasing tube voltage to 100 kVp, Radiology 266(3) (2013) 791-800.

[25] Y. Nakayama, K. Awai, Y. Funama, D. Liu, T. Nakaura, Y. Tamura, Y. Yamashita, Lower tube voltage reduces contrast material and radiation doses on 16-MDCT aortography, AJR Am J Roentgenol 187(5) (2006) W490-7.

[26] T. Nakaura, Y. Nagayama, M. Kidoh, S. Nakamura, T. Namimoto, K. Awai, K. Harada, Y. Yamashita, Low contrast dose protocol involving a 100 kVp tube voltage for hypervascular hepatocellular carcinoma in patients with renal dysfunction, Jpn J Radiol 33(9) (2015) 566-76.

[27] Y. Noda, M. Kanematsu, S. Goshima, H. Kondo, H. Watanabe, H. Kawada, N. Kawai, Y. Tanahashi, T.R.T. Miyoshi, K.T. Bae, Reducing iodine load in hepatic CT for patients with chronic liver disease with a combination of low-tube-voltage and adaptive statistical iterative reconstruction, Eur J Radiol 84(1) (2015) 11-18.

[28] M.H. Yu, J.M. Lee, J.H. Yoon, J.H. Baek, J.K. Han, B.I. Choi, T.G. Flohr, Low tube voltage intermediate tube current liver MDCT: sinogram-affirmed iterative reconstruction algorithm for detection of hypervascular hepatocellular carcinoma, AJR Am J Roentgenol 201(1) (2013) 23-32.

[29] T. Ichikawa, U. Motosugi, H. Morisaka, K. Sano, M. Ali, T. Araki, Volumetric low-tube-voltage CT imaging for evaluating hypervascular hepatocellular carcinoma; effects on radiation exposure, image quality, and diagnostic performance, Jpn J Radiol 31(8) (2013) 521-9.

[30] S. Hur, J.M. Lee, S.J. Kim, J.H. Park, J.K. Han, B.I. Choi, 80-kVp CT using Iterative Reconstruction in Image Space algorithm for the detection of hypervascular hepatocellular carcinoma: phantom and initial clinical experience, Korean J Radiol 13(2) (2012) 152-64.

[31] C.H. Lee, K.A. Kim, J. Lee, Y.S. Park, J.W. Choi, C.M. Park, Using low tube voltage (80kVp) quadruple phase liver CT for the detection of hepatocellular carcinoma: two-year experience and comparison with Gd-EOB-DTPA enhanced liver MRI, Eur J Radiol 81(4) (2012) e605-11.

[32] V. Chernyak, K.J. Fowler, A. Kamaya, A.Z. Kielar, K.M. Elsayes, M.R. Bashir, Y. Kono, R.K. Do, D.G. Mitchell, A.G. Singal, A. Tang, C.B. Sirlin, Liver Imaging Reporting and Data System (LI-RADS)

Version 2018: Imaging of Hepatocellular Carcinoma in At-Risk Patients, Radiology 289(3) (2018) 816-830.

[33] D.P. Chakraborty, X. Zhai, Analysis of Data Acquired Using ROC Paradigm and Its Extensions, https://mran.microsoft.com/snapshot/2015-05-08/web/packages/RJafroc/vignettes/RJafroc.pdf accessed Oct/2021 (2015).

Tables

Figures

Figure 3 Hepatocellular carcinoma on computed tomography during arteriography at the first phase in a 66-year-old female patient

The enhanced lesion in the right lobe is unclear on the 135 kVp image (a: arrow), whereas it is well-delineated on the 80 kVp image (b: arrow). Compared to the 135 kVp image (a: asterisk), contrast enhancement of the protruded large tumor in the lateral segment is increased in the 80 kVp image (b: asterisk). Two of three readers rated the same confidence scores (90 and 100 for the 135 kVp and 80 kVp images, respectively), whereas the other reader's confidence scores were improved from 50 for the 135 kVp image to 60 for the 80 kVp image.

Figure 4 Free-response receiver operating characteristic curve

Lesion localization fraction (LLF) is defined as the cumulative number of lesion localizations divided by the total number of lesions. Non-lesion localization fraction (NLF) is defined as the cumulated number of non-lesion localizations divided by the total number of cases. The plots show the confidence scores the readers rated. Note the difference of scale in the x-axis. The maximum LLFs were higher in the 80 kVp images for two of three readers but similar to the 135 kVp in one of three readers. The maximum value of the curves of the 80 kVp image is larger and greater than 1.0 for two of three readers.

a, Reader 1; b, Reader 2; c, Reader 3.

Figure 5 Comparison of scores in evaluating the liver parenchyma and detecting hepatocellular carcinoma

Comparison scores in evaluating liver parenchyma are represented by gray bars and those in detecting hepatocellular carcinomas (HCC) by black bars. Significant differences were observed in one of three readers in both liver parenchyma ($P = 0.035$) and HCCs ($P = 0.018$), using the Wilcoxon signed-rank test. The results of Reader 1 and Reader 2 demonstrate the tendency toward a trade-off relationship between liver parenchyma and HCC assessment.

a, Reader 1; b, Reader 2; c, Reader 3.

Acknowledgements

The authors would like to thank Enago (www.enago.jp) for the English language review.

Credit Author Statement

Akitoshi Inoue: Conseptualization, Methodology, Formal analysis, Writing – Original Draft, **Ryo Uemura**: Investigation, **Kai Takaki**: Investigation, **Akinaga Sonoda**: Investigation, **Norihisa Nitta**: Conseptualization, Writing - Review & Editing, **Shinichi Ota**: Investigation, Validation, **Bolorkhand Batsaikhan**: Investigation, **Hiroaki Takahashi**: Methodology, Formal analysis **Yoshiyuki Watanabe**: Supervison

Table 1 Likert scores for subjective image quality analysis

Overall image quality
1 = nondiagnostic due to excessive noise or artifacts
2 = diagnosis questionable, moderate decrease in confidence
3 = diagnostic with moderate but acceptable noise or artifacts
4 = mild noise, no change in confidence
5 = routine diagnostic image quality
Artifacts
1 = Severe artifacts, confidence degraded, diagnosis questionable
2 = Major artifacts, affecting the visualization of normal structures
3 = Mild artifacts, not affecting the visualization of any structure
4 = No artifacts, high confidence in diagnostic capability
Sharpness
1 = Noticeable blur
2 = Questionable, but adequate for diagnosis
3 = Very sharp
Noise
1 = noise affects interpretation compared to routine clinical
2 = Optimal noise
3 = Less than usual

Table 2 Patient characteristics

Age (year, SD)		74.4 (8.0)
Sex (%)		
	Male	17 (73.9)
	Female	6 (26.1)
Body mass index (kg/m^2, SD)		23.6 (2.6)
Iodine per body weight (mgI/kg, SD)		38.7 (6.5)
Number of HCCs (%)		
	One	3 (13.0)
	Two	5 (21.7)
	Three	7 (30.4)
	Four	1 (4.3)
	Five	1 (4.3)
	Six	2 (8.7)
	Seven	1 (4.3)
	Eight	1 (4.3)
	Nine	1 (4.3)
	Ten	1 (4.3)

Table 3 Sensitivity and positive predictive value with 95% confidence interval in 135kVp and 80kVp images

	Sensitivity		Positive predictive value	
	80 kVp	135 kVp	80 kVp	135 kVp
R1	0.831 (0.737—0.903)	0.730 (0.626—0.819)	0.712 (0.615—0.800)	0.783 (0.679—0.866)
R2	0.764 (0.662—0.848)	0.787 (0.687—0.866)	0.673 (0.573—0.763)	0.729 (0.629—0.815)
R3	0.764 (0.662—0.848)	0.674 (0.567—0.770)	0.756 (0.654—0.840)	0.759 (0.650—0.849)
Overall	0.787 (0.732—0.834)	0.730 (0.673—0.783)	0.712 (0.657—0.763)	0.756 (0.657—0.768)

Table 4 Results of subjective image quality analysis

	80 kVp	135 kVp	P value
Sharpness			
R1	2.3 ± 0.5	2.1 ± 0.3	0.008*
R2	2.5 ± 0.5	2.6 ± 0.6	0.774
R3	1.8 ± 0.7	1.8 ± 0.7	1.000
Artifact			
R1	3.0 ± 0.2	3.0 ± 0.2	1.000
R2	3.3 ± 0.6	3.7 ± 0.5	0.056
R3	2.8 ± 0.5	3.0 ± 0.6	0.273
Noise			
R1	2.1 ± 0.3	2.7 ± 0.5	0.002*
R2	2.0 ± 0.0	2.2 ± 0.4	0.063
R3	1.8 ± 0.6	2.1 ± 0.5	0.246
Overall image quality			
R1	3.8 ± 0.4	4.0 ± 0.3	0.219
R2	4.6 ± 0.6	4.4 ± 0.6	0.337
R3	3.6 ± 0.8	3.8 ± 0.5	0.373

Wilcoxon signed-rank test *: $P<0.05$

Table 5 Lesion-liver contrast ratio and objective noise

		80 kVp	135 kVp	P value
Lesion-to liver-contrast ratio				
	1st phase	3.1 ± 3.4	2.0 ± 1.6	0.008*
	2nd phase	3.1 ± 2.9	2.3 ± 1.3	0.016*
Noise				
	1st phase	15.6 ± 5.2	3.1 ± 1.6	<0.001*
	2nd phase	16.9 ± 5.2	15.0 ± 1.3	0.046*

Paired t-test *: $P<0.05$

Figure.1

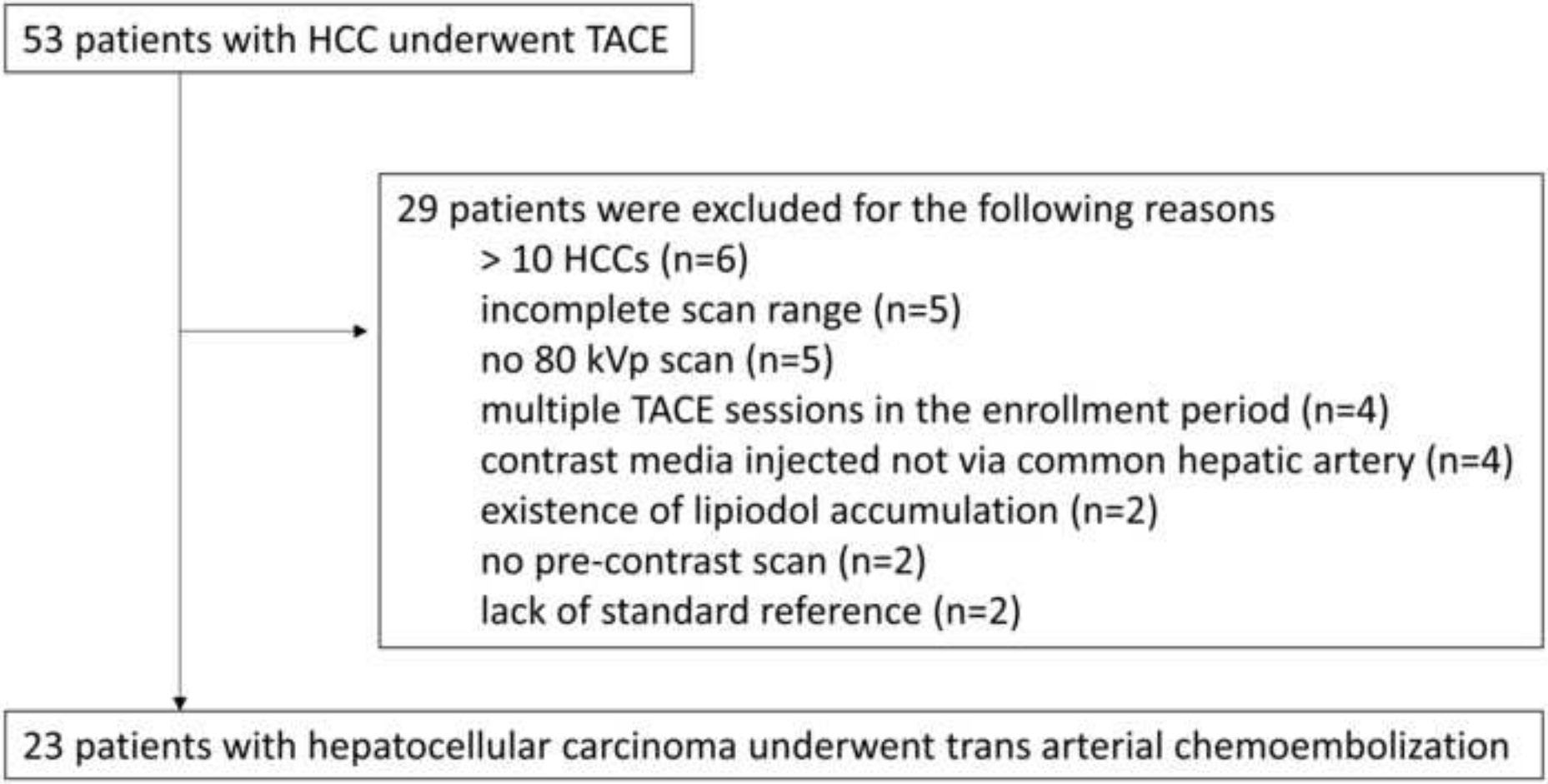

Figure.2

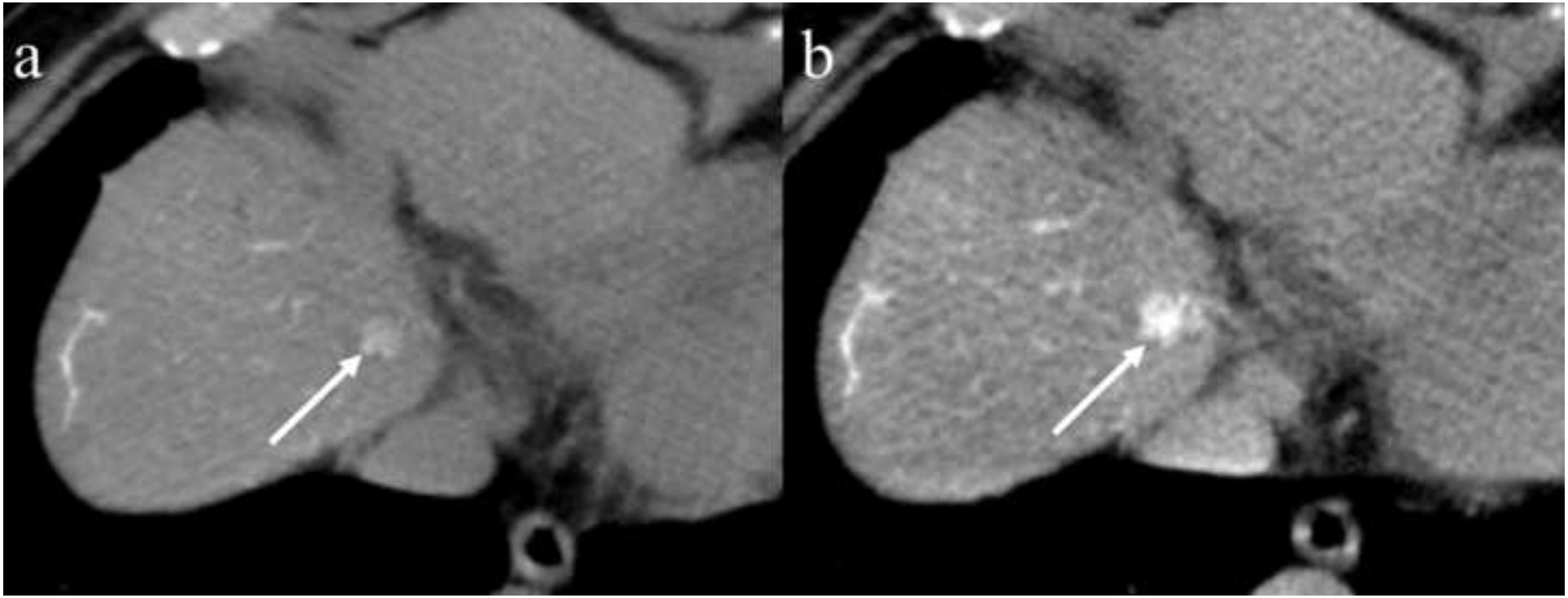

Figure.3

Click here to access/download;Figure(s);Fig3.TIF

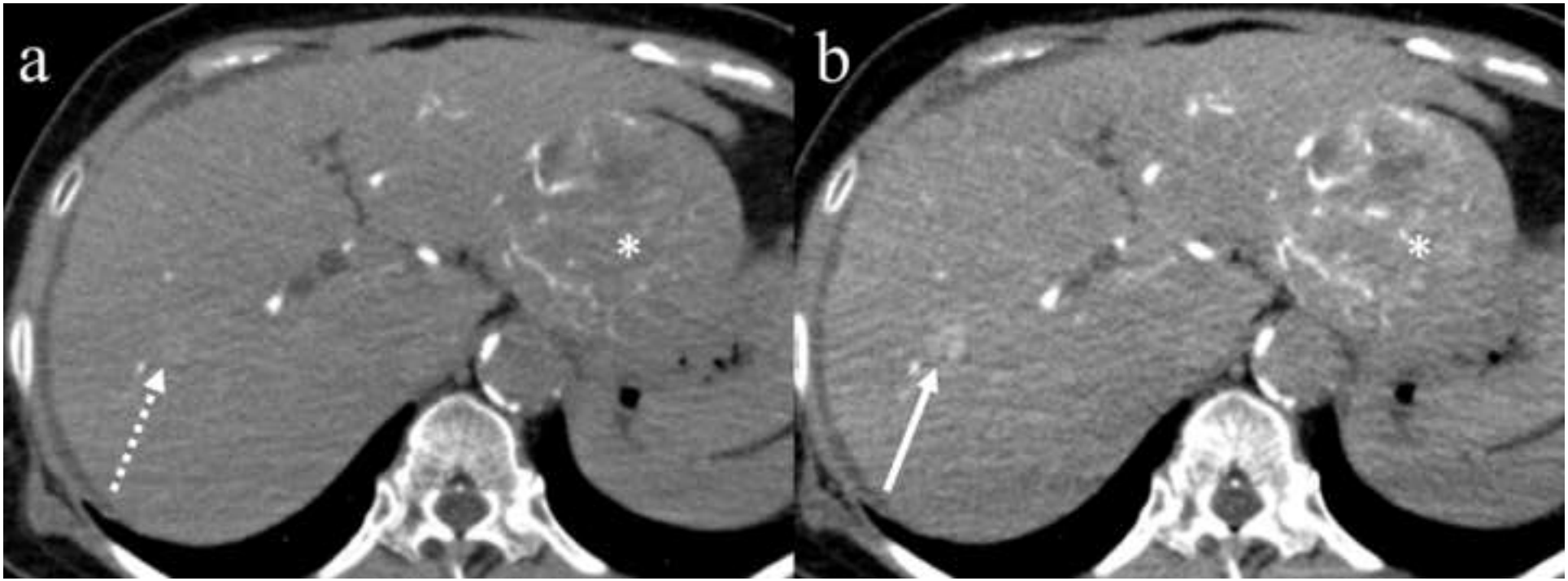

Figure.4

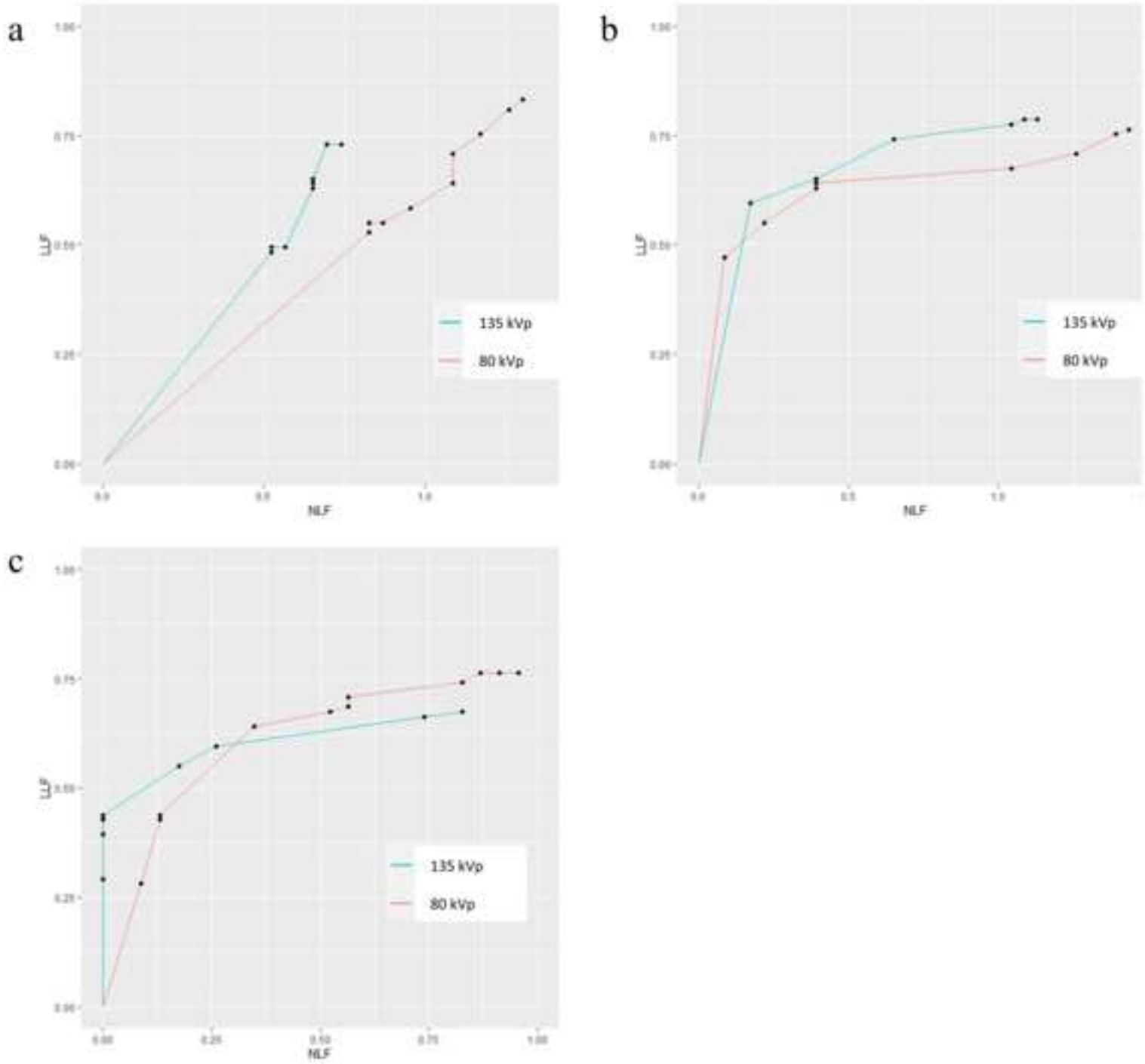

Figure.5